

Bilateral Decoupling in the Neural Control of Biped Locomotion

Chandana Paul

Artificial Intelligence Laboratory
University of Zurich
Winterthurerstr. 190, CH-8057 Zurich, Switzerland
chandana@ifi.unizh.ch

Abstract

In this paper, a bilaterally decoupled neural controller was used to achieve stable locomotion in a 6 DOF biped robot with 5 links, implemented in a virtual physics-based simulation environment. The neural controller consists of an independent neural rhythm generator for each leg. The rhythm generator is a recurrent neural network, whose weights are optimized by a genetic algorithm and are identical for both legs. Each one receives inputs only from its own joint angle sensors and touch sensor on the foot, and produces motor commands for joints of the same leg. However, by using sensory feedback from the mechanical coupling of the legs through the body, they can synchronize to produce coordinated stepping movements. Furthermore, improvements in the quality of the gait can be achieved only with global sensory information. The results suggest the possibility that there may not be a need for explicit contralateral sensory coupling or neural connections in bipedal locomotion.

1 Introduction

Neural control of human locomotion is not yet fully understood. There is strong evidence which suggests that isolated neural circuits called central pattern generators exist in vertebrates to produce rhythmic oscillatory patterns, which coupled with the dynamics of the body produce locomotion. Experiments with cats have shown that a decerebrated cat can walk on a treadmill when some parts of the brain stem are stimulated [10]. It has also been shown that even in the complete absence of stimulus neural circuits exist in the spinal cord which can produce oscillatory motor outputs [4].

Similar results have been found in humans. In experiments with newborn infants it has been shown that they are capable of producing stepping movements when they are held upright [12]. Also, in experiments with complete adult paraplegic patients, it is shown that they are able to produce stepping movements when supported on a moving treadmill [3]. These results suggest that the same neural circuits which are capable of autonomous rhythm generation in vertebrates may be involved in human bipedal locomotion.

Although computational studies have shown that small neural circuits consisting of 2-6 mutually inhibiting neurons are capable of such autonomous rhythm generation [7], the half-center hypothesis of central pattern generation [2] is most prevalent for vertebrates. This proposes that small neural units of two reciprocally inhibited "half-center" neurons are responsible for rhythm generation in each joint.

The half-center model of a CPG has been implemented by Matsuoka as a set of differential equations [6], which has been widely used in studies of rhythmic movement generation. Kimura *et al* [5] developed a neural controller for a quadruped robot, consisting of one such CPG for each of the hip and knee joints. The hip CPGs were connected to each other so that diagonal legs were paired. Taga used the Matsuoka oscillator in a similar neural controller for biped locomotion, with a single CPG connected to the flexor and extensor muscles of each of the hip, knee and ankle joints. [11]. In this model, explicit phase dependent connections were introduced between the ipsilateral oscillators, and permanent inhibitory connections were implemented between contralateral oscillators of each joint to ensure phase-locking in an anti-phase relationship. However, in a model of arm control using CPGs it was shown that phase-locking could occur only by sensing of mechanical coupling [13].

In this paper, the goal was to investigate whether explicit contralateral connections, as used in the previous studies on biped locomotion, are necessary for phase-locking. It was hypothesized that the mechanical coupling of the legs through the body could be sufficient to coordinate the movements of the two legs. To test this, an independent neural rhythm generator was used for each leg of a 6 DOF biped robot. The rhythm generator was a recurrent neural network with one hidden layer, which only received sensory inputs from one side of the body. The weights of the network were optimized using a genetic algorithm, as in the work of Ogihara *et al* [8], but the search space was additionally improved using morphological parameters [1]. Two different neural architectures were tested: one with complete bilateral decoupling, where only sensory information related to the legs was available to each rhythm generator, and another in which global sensory information related to body attitude was also provided. It was shown that in both cases, the legs were able to coordinate despite the absence of explicit neu-

Table 1: Morphological parameters of the biped robot. A ul represents one unit length defined as the five times the radius of the spherical sockets at the hip and knees. A um represents one unit mass defined as the mass of the same spherical socket. The ranges of the parameters which vary under evolutionary control are shown in square brackets.

Index	Object	Dimensions	Mass
1	Knees	$r = 0.2 \text{ ul}$	1 um
2	Hip sockets	$r = 0.2 \text{ ul}$	1 um
3	Feet	$r = 0.4 \text{ ul}, w = 0.8 \text{ ul}$	1 um
4	Lower Legs	$r = [0.04, 0.16] \text{ ul}, h = 8 \text{ ul}$	$[0.1, 0.4] \text{ um}$
5	Upper Legs	$r = [0.04, 0.16] \text{ ul}, h = 8 \text{ ul}$	$[0.1, 0.4] \text{ um}$
6	Waist	$r = [0.04, 0.16] \text{ ul}, w = 8 \text{ ul}$	$[0.1, 0.4] \text{ um}$

Index	Joint	Plane of Rotation	Range of Motion
10	Knee	sagittal	$-\frac{\pi}{2} \rightarrow 0$ (radians)
11	Hip	sagittal	$-\frac{\pi}{7} \rightarrow \frac{\pi}{7}$
12	Hip	frontal	$-\frac{\pi}{10} \rightarrow \frac{\pi}{12}$

ral connections and produce stable walking.

The following sections, describe the biped robot (Section 2), the neural controllers with bilateral decoupling and global sensing (Section 3) and the genetic algorithm (Section 4). Section 6 presents the main results of the experiments, followed by Section 7 which discusses the results. Section 8 summarizes with conclusions.

2 The Robot

The robot is a 5-link biped robot with 6 degrees of freedom, simulated in a real-time, physics-based virtual environment¹. The robot has a waist, two upper leg and two lower leg links as shown in Fig 1. Each knee joint, connecting the upper and lower leg links, has one degree of freedom in the sagittal plane. Each hip joint, connecting the upper leg to the waist, has two degrees of freedom: one in the sagittal plane and one in the frontal plane. These correspond to the pitch and roll motions.

The joints are limited in their motion with joint stops, with ranges of motion closely resembling those of human walking. The hip pitch joint on each side has a range of motion between $-\pi/7$ and $\pi/7$ degrees with respect to the frontal plane. The hip roll joint has a range of motion between $-\pi/12$ and $\pi/12$, with respect to the sagittal plane. The knee joint has a range of motion between $-\pi/2$ and 0 with respect to the axis of the upper leg link to which it is attached.

Each of the joints is moved by a simulated torsional actuator. The actuator receives position commands from the controller. It uses proportional control to determine the velocity of the link, with a relatively low maximum torque ceiling. The torque applied to actuators is determined by

$$\tau_{t+1} = \max(I(\omega_t - k(\theta - \theta_d)), \tau_{max}) \quad (1)$$

where θ is the actual joint angle, θ_d is the desired joint angle, τ_{max} is the maximum torque ceiling, $\omega = \dot{\theta}$, and I is the feedback gain matrix.

¹MathEngine PLC, Oxford, UK, www.mathengine.com

This means that the velocity of a link will be greater the further it is from the commanded joint angle position, but if the force required to achieve this velocity is too large, it will only apply the maximum force. This mechanism incorporates a measure of compliance into the system, and is in accordance with the capabilities of real world actuators.

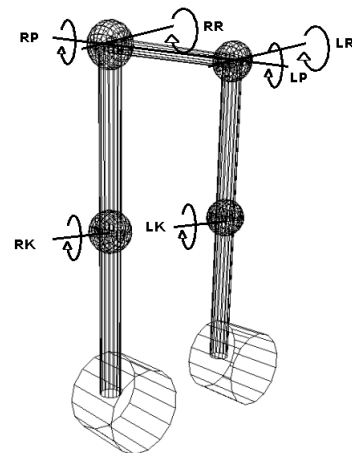


Figure 1: The biped physical structure and its six degrees of freedom. The labels indicate the joint angle and foot contact sensors. The widths of the biped links vary under evolutionary control within the range shown in Table 1.

3 Neural Controller

3.1 Complete Bilateral Decoupling

For the investigation of complete bilateral decoupling, a neural controller was designed with an independent identical neural rhythm generators for each leg (Fig. 2). Each rhythm generator was a recurrent neural network consisting of an input layer with sensory input nodes and a bias neuron, a hidden layer of 4 nodes with lateral connections and a second bias neuron, and an output layer with motor outputs.

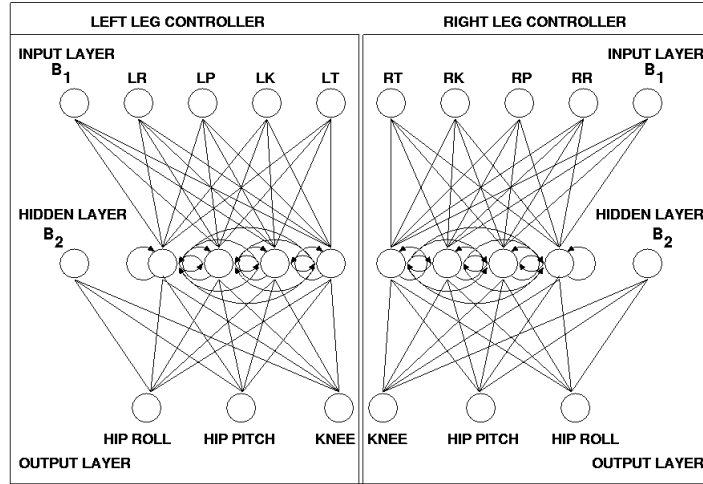


Figure 2: Bilaterally decoupled neural controller including only joint angle and foot contact sensors. The input nodes for the left leg controller are LR: Left Hip Roll, LP: Left Hip Pitch, LK: Left Knee Pitch, LT: Left foot contact and the outputs are to the left hip roll, hip pitch and knee joints. For the right leg controller the inputs are RR: Right Hip Roll, RP: Right Hip Pitch, RK: Right Knee Pitch, RT: Right Foot Contact and the outputs are to the right hip roll, hip pitch and knee joints. B_1 and B_2 are bias nodes.

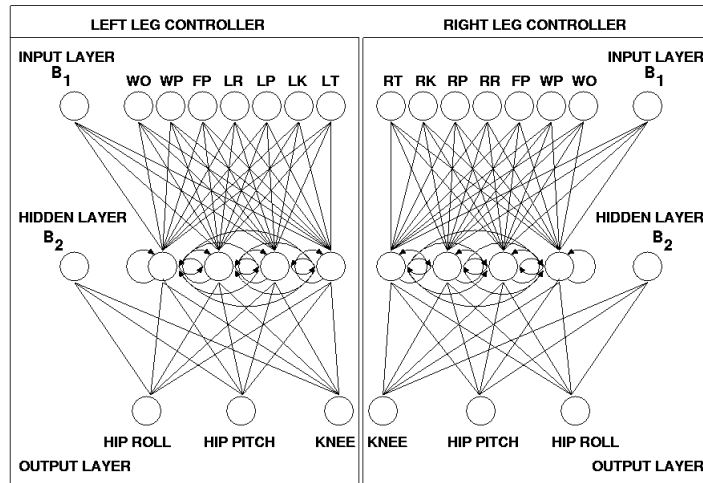


Figure 3: Bilaterally decoupled neural controller enhanced with global sensing. In addition to the nodes in the bilaterally decoupled controller in Figure 2, the left leg controller has sensory input nodes for WO: waist orientation in transverse plane, WP: waist sagittal position and FP: left foot sagittal position. For the right leg controller the input to FP is the foot position of the right foot instead.

The sensory inputs of the network were from the biped robot. The biped has proprioceptive sensors at each joint whose values are scaled to the range $[-1, 1]$. It also has haptic sensors on the feet, which outputs 1 if the foot is in contact with the ground and -1 otherwise. It is actuated by torsional actuators attached to the six joints. Thus, the neural rhythm generators have 4 input nodes, one for each of the three proprioceptive sensors and one for the haptic sensor of a leg. They have 3 output nodes, one for each of the actuated joints of the same leg. The input layer is fully connected to a hidden layer. The hidden layer is fully and recurrently connected, plus an additional bias neuron.

The hidden and bias neurons are fully connected to the three neurons in the output layer. All neurons in the network emit a signal between -1 and 1 . Bias neurons constantly emit a signal of 1. The activations of the hidden and output neurons are computed by

$$a = \sum_{i=1}^n w_{ij} O_i \quad (2)$$

where O_i is the output of a neuron in the previous layer. In the hidden layer, however, O_i represents both the output from the input layer at the current time step, and the output

from the hidden layer at the previous time step. w_{ij} is the weight of the synapse connecting them. The output of this neuron is then given by

$$O = \frac{2}{1 + e^{-a}} - 1 \quad (3)$$

The values at the output layer are scaled to fit the range of their corresponding joint's range of motion. Torsion is then applied at each joint to attain the desired joint angle.

The recurrent structure of the hidden layer in the rhythm generator allows for lateral inhibition and thus the intrinsic capability of producing cyclic dynamics. The rhythm generator closely mimics the structure of the monolithic neural controller used in previous work by Paul *et al*[9] for the evolution of biped walking. This controller received inputs from all joint angle and foot contact sensors in the same network, passed it on to a recurrent hidden layer with 3 nodes, which then passed it on to the output layer with six outputs, one for each joint of the biped. The current network can be visualized as the monolithic network "cut in half" (with a few more nodes added to the hidden layer).

The single leg neural rhythm generator can also be considered a simplified version of the ipsilateral leg controller used by Taga [11]. It allows for cyclic dynamics, but with reduced flexibility in the phase relationships between the joints, as there are fewer oscillatory units and the connections in the controller are permanent and not phase dependent. However, as the focus of this study was not ipsilateral but contralateral coupling, the complexity of the network was sufficient.

3.2 Bilateral Decoupling with Global Sensing

As the mechanical coupling of the legs determines that movement of either leg will influence global variables corresponding to body attitude, it was hypothesized that including such global sensory information in the network could improve the stability of the gait pattern. Thus, for this test the network described in the previous section was augmented with three new sensory inputs (Fig. 3). A global sensor of the orientation of the waist in the transverse plane (WO) was added, to detect deviations of the biped from a straight line path. As the evaluation of a biped was terminated if the biped veered more than 0.9 radians from its initial orientation, the orientation sensor produced a signal between in the range [0.0, 0.9]. Two more sensors were included for the foot sagittal position (FP) and waist sagittal position (WP), so if necessary the network could compute the difference between the two, and use it to detect the phase of the gait cycle. These sensors produced output values proportional to position without further normalization. Both the right and left networks were given the three sensor values as additional inputs, so the input layer consisted of seven input nodes instead of four. As the networks were identical, the global sensor values were multiplied by the same connections weights on both sides, and had the same effect on right and left rhythm generators.

3.3 Initial Condition

At the beginning of the simulation all the joint angles and velocities of the biped are 0, and both haptic sensors are 1.

Thus, the sensory inputs of the right and left rhythm generators are identical. As the weights of the two rhythm generators are also identical, identical outputs are produced. This could only lead to two situations: standing in place or hopping, which are the two behaviors in which both legs perform identical movements. It would not lead to walking, as the start of walking is an asymmetric motion: one leg enters swing phase as the other one stays on the ground. Thus, the control of the start of walking had to be performed externally to the network. In other words, the initial conditions had to be determined so that the network would function. As the initial conditions are closely coupled to the performance of the network, which is determined by the weights set by the genetic algorithm, it was also necessary to let the genetic algorithm control the initial conditions. Thus, the initial motor commands for the actuators of the biped in the first 10 steps of the simulation are six values generated by the genetic algorithm. The network takes control of the biped after this time has elapsed.

4 The Genetic Algorithm

A fixed length genetic algorithm was used to evolve the controllers. Each run of the genetic algorithm was conducted for 300 generations, using a population size of 200.

At the end of each generation, the 100 most fit genomes were preserved; the others were deleted. Tournament selection with a tournament size of three, is employed to probabilistically select genotypes from among those remaining for mutation and crossover. 25 pairwise one-point crossings produce 50 new genotypes: the remaining 50 new genotypes are mutated copies of genotypes from the previous generation. The mutation rate was set to generate an average of seven mutations for each new genome created. Mutation involved the replacement of a single value with a new random value. Each genome contains floating-point values which are rounded to two decimal places and range between -1.00 and 1.00 . In the optimization of the fully bilaterally decoupled neural controller the genome encodes 51 synaptic weights of the neural network, 3 morphological parameters to determine the link widths, and 6 initial position commands, and thus has a total length of 60 parameters. In the controller with global sensing the number of synaptic weights increases to 63, and the genome length to 72, due to the three additional input nodes.

During evolution each individual is evaluated for 2000 time steps of the dynamics simulation. The initial condition for each individual at the first time step is one in which all joint angles and velocities are set to zero. This results in a fully upright posture, with all parts aligned in the frontal plane, and both feet at an equal distance from the target. The evaluation is prematurely terminated if the center of gravity of the waist drops below the original vertical position of its knees (it falls) or if it "twists" too much, or if both feet lift off the ground, (it starts to run). This third termination criteria was added because the primary interest of this project was to study walking, and not running gaits. At the end of the evaluation, the distance of the biped traveled in the sagittal plane (determined relative to its original position) is

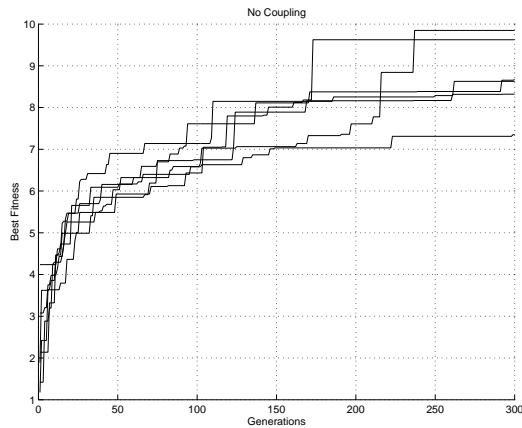


Figure 4: Best fitness in each generation, for the six evolutionary optimization experiments with complete bilateral decoupling.

considered its fitness.

5 Results

Six full evolutionary optimizations were performed for the fully bilaterally decoupled controller, and the decoupled controller with global sensing. Each optimization ran for approximately 3.5 hours on a 1 GHz Pentium III PC. Thus, the results presented below are from approximately 40 hours of data collection.

5.1 Complete Bilateral Coupling

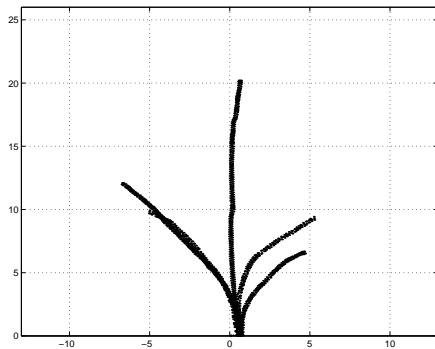


Figure 5: Trajectories of the most successful bipeds in each of the six experiments. (Some of the trajectories overlapped.)

In the experiments with complete bilateral decoupling, five out of six runs evolved stable gait cycles. The history of the best fitness in each of the experiments is shown in Figure 4. The final fitness in all the experiments fell in a small range approximately between 7 and 10 ul. The gait was very similar in all these cases. An almost straight legged walking evolved with very small step size, using the rocking motion afforded by the cylindrical feet for ground clearance. The gait was very stable; although the controller was evolved to

function for only 2000 time steps of the dynamic simulation, even after 5000 time steps most of the bipeds continued to walk, indicating that they had achieved a stable limit cycle. However, the trajectories often veered off sideways as shown in Fig 5. Out of the five successful walkers, two had trajectories which twisted too much and therefore were prematurely terminated, with a low fitness. The three others, also had trajectories which veered off the straight line path to a certain extent although not enough to be terminated. The average fitness therefore after 5000 time steps of all the experiments was 15.6, although the best was 24.34.

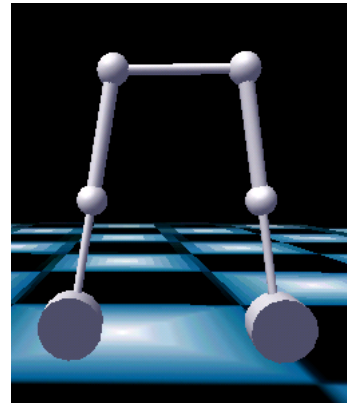


Figure 6: Physical Structure of the biped which achieved the highest fitness with complete bilateral decoupling.

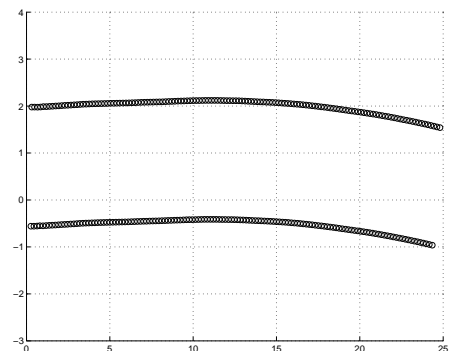


Figure 7: Foot placement history of the biped with highest fitness. Each footprint is represented by a \circ .

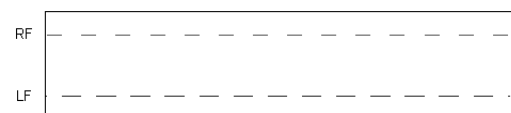


Figure 8: Footsteps of the biped with highest fitness. Dark lines indicate that the foot is in contact with the ground. The length of the line indicates the duration of time for which the foot was in contact with the ground in one step.

The best agent evolved in this set of experiments is shown in Figure 6. It had a lower leg width of 0.056 ul, an upper leg width of 0.097 ul, and a waist width of 0.62 ul. It used initial joint angle positions of $[-0.57, 0.50, 0.62, 0.21, 0.10, 0.93]$ for the left knee, left hip roll, left hip pitch, right hip pitch, right hip roll and right knee joints respectively. Figure 7 shows this biped's foot placement history. It can be seen that its trajectory is slightly curved, although there are long periods of stable alternating stepping. In Figure 8 the length of time during which each foot is in contact with the ground is plotted. It can be seen that its step duration is basically symmetric and alternates regularly although the left foot is in contact with the ground for slightly longer time intervals than the right foot. This asymmetry could be a consequence of the particular initial conditions set by evolutionary algorithm for this biped.

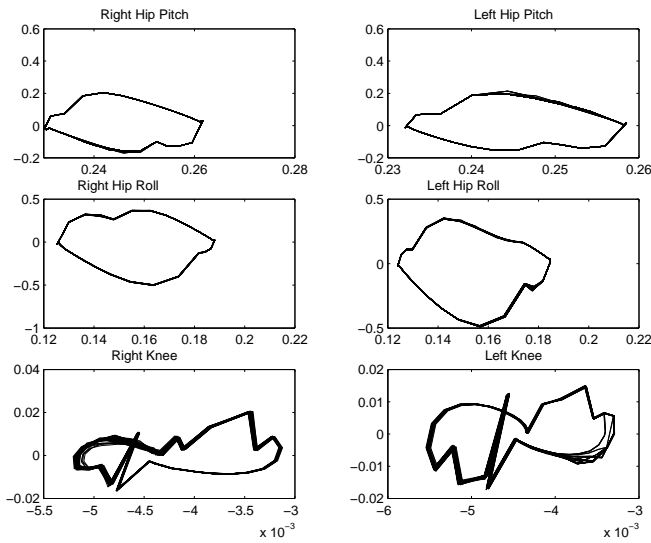


Figure 9: Steady state phase plots of the joint angles of the biped with highest fitness. The x-axis plots θ and the y-axis $\dot{\theta}$.

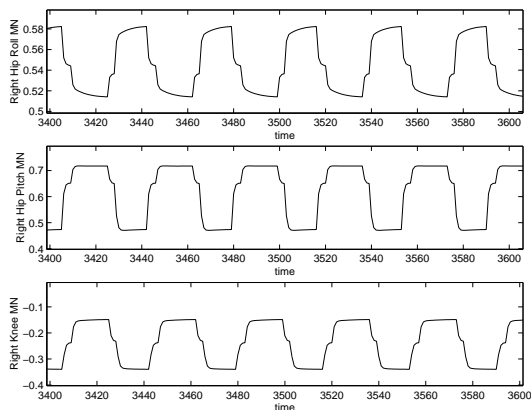


Figure 10: Motor Neuron Activations of the Right Hip Pitch, Hip Roll and Knee joints, of the biped with highest fitness.

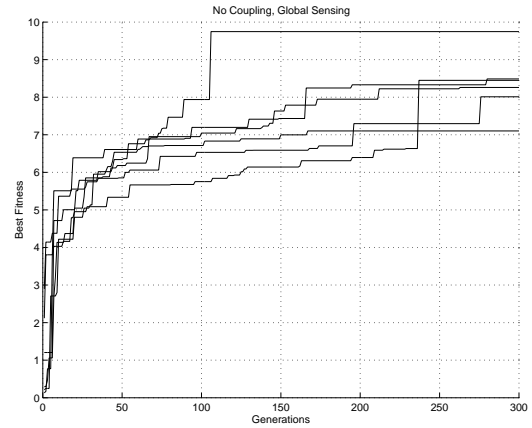


Figure 11: Best fitness in each generation, for the six evolutionary optimization experiments on bilateral decoupling with global sensing.

The measure of stability of this biped's gait can be gauged in the steady state phase plots of the joint angles shown in Figure 9. The phase plots of the pitch and roll degrees of freedom at both hip joints show closed orbits with a high degree of regularity indicating a stable limit cycle. The knee phase plots also have closed orbits but they are more irregular and a closer look at the $\dot{\theta}$ axis indicates that the orbits span a very limited range of positions and velocities close to zero, indicating that the knees did not move much at all. It basically seems that the controller actively locked the knee at 0° , in order to use the straight-legged gait. Figure 10 shows the motor neuron activity for the three joints of the right leg. All three motor neurons show regular oscillatory patterns also indicative of a stable limit cycle.

5.2 Bilateral Decoupling with Global Sensing

In this set of experiments, the fitness graphs after 300 generations were similar to the case of complete bilateral decoupling as seen in Figure 11. However, on running each of the bipeds for 5000 time steps it was found that *all* of them had evolved stable walking. Moreover, the bipeds had achieved a high degree of directional control so that most of the trajectories were more or less straight, as seen in Figure 12. The gaits evolved were quite similar to those observed in the previous set of experiments: straight legged walking with small step size and rocking for ground clearance. However, since the trajectories were all straight, none of the runs had to be prematurely terminated. This yielded a high average fitness of 19.14, with a best fitness of 25.1.

The best agent evolved in this set of experiments, had lower leg width 0.057 ul, upper leg width 0.1 ul, and waist width 0.13 ul as shown in Figure 13. It used initial joint angle positions of 0.00, -0.03, 0.62, -0.78, 0.61, and 0.00 for the left knee, left hip roll, left hip pitch, right hip pitch, right hip roll and right knee joints respectively. Figure 14 shows the bipeds foot placement history over 5000 time steps. It can be seen here that after a transient phase where the foot placement is irregular the biped settles down into a stable straight line trajectory. Figure 15 shows the corresponding

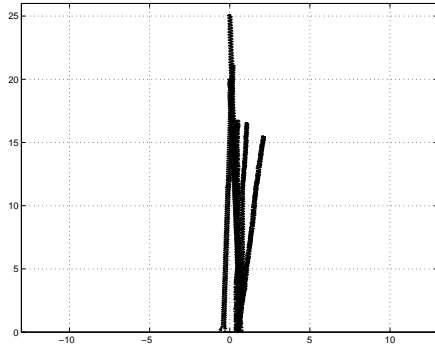


Figure 12: Trajectories of the most successful bipeds in each of the six experiments. (Some of the trajectories overlapped.)

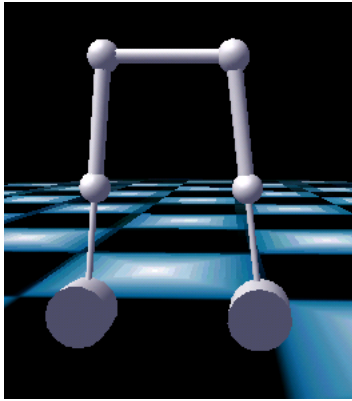


Figure 13: Physical Structure of the biped which achieved the highest fitness with bilateral decoupling and global sensing.

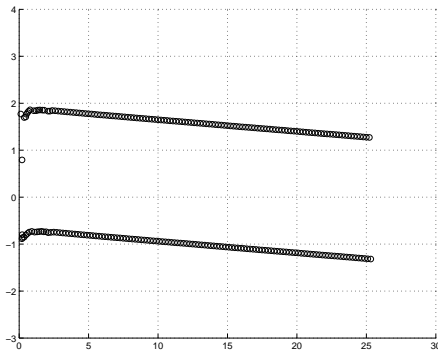


Figure 14: Foot placement history of the biped with the highest fitness. Each footprint is represented by a \circ .

foot step durations of the biped during a brief time interval. As in the previous case the foot steps are regularly alternating in time. It is interesting that once again there is a slight bias towards the left foot being on the ground longer than the right. However, in this case the difference is smaller.

The stability of the limit cycle is once again quite high

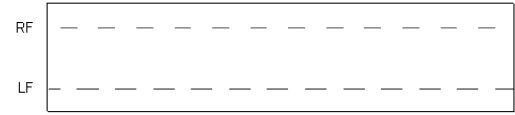


Figure 15: Footsteps of the biped with the highest fitness. Dark lines indicate that the foot is in contact with the ground. The length of the line indicates the duration of time for which the foot was in contact with the ground in one step.

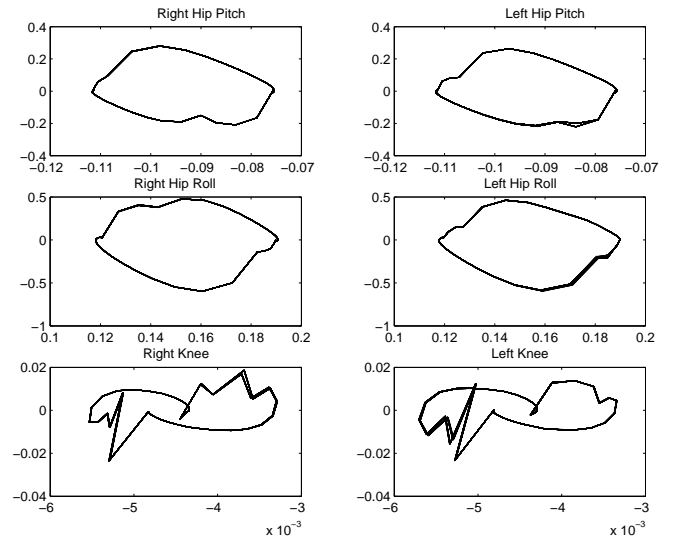


Figure 16: Steady state phase plots of the joint angles of the biped with highest fitness. The x-axis plots θ and the y-axis plots $\dot{\theta}$.

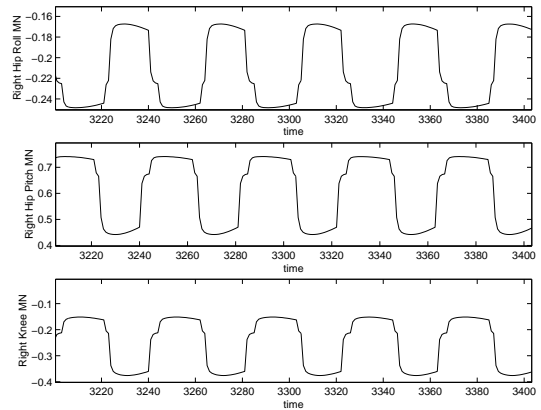


Figure 17: Motor Neuron Activations of the Right Hip Pitch, Hip Roll and Knee joints of the best biped with highest fitness.

for all the joints, as observed in Figure 16. The stability of the hip pitch and roll limit cycles is comparable to the case of complete bilateral decoupling. The knee limit cycle is more stable in this case. The motor neuron outputs shown

in Figure 17 have a more rounded shape compared to those of the biped with complete bilateral decoupling. It seems that the global sensing allowed the controller to improve the smoothness of the motor neuron outputs and increase the stability of the gait.

6 Discussion

The results showed that a bilaterally decoupled neural controller could lead to synchronized motions of the right and left legs to produce to stable locomotion in a 6 DOF biped, using mechanical coupling. Furthermore, the directionality and stability of the gait could be improved without the need for explicit connections, only using global sensing. The question arises of whether such a neural architecture could be biologically plausible for human locomotion. It is certainly more plausible than an architecture which was found to be equally successful in previous experiments (whose results could not be presented here due to space constraints) in which two identical neural rhythm generators each received sensory inputs from sensors on both left and right sides. The current network achieves almost identical performance with much fewer afferent connections. However, the question of whether such a neural architecture is more biologically plausible than a controller with explicit connections in the neural controller, is more difficult to answer. As all the oscillatory units are believed to be located in the spinal cord, it is likely to be relatively cheap for the system to have connections between them if it leads to greatly increased stability and robustness. It would be necessary to perform further tests of robustness on decoupled controllers to determine whether bilateral coordination through mechanical coupling and global sensing is equivalent, inferior to, or superior to having explicit neural connections in the controller.

Another issue is that in the experiments, the bipeds have cylindrical feet oriented parallel to the sagittal plane, enabling them to exploit the rocking motion for foot clearance. Although it would be desirable to have a more human-like gait, the straight legged walking does not in itself reduce the biological plausibility of the neural architecture, as the anti-phase relationships already sensed for the hip movements through mechanical coupling could be propagated via ipsilateral connections to the knees and ankles.

However, in these experiments the biped has 6 DOF and rigid ankles, as compared to 12 DOF or more in the human lower body. Also, the motoneuron outputs are used to control desired angle and not muscle force. Thus, it is a highly simplified biorobotic platform. To make a stronger bid for biological plausibility the results will have to be extended to a more anthropomorphic simulation in future investigations.

7 Conclusions

In this paper it is shown that a bilaterally decoupled neural controller, consisting of two identical neural rhythm generators which each receive sensory inputs from one side of the body, is capable of producing stable locomotion in a 6 DOF biped robot in simulation. The bilateral coordination is achieved via sensing of the mechanical coupling of the legs through the body, to achieve stable straight-legged

locomotion. Directional control can be improved only using global sensing. These results are in contrast to previous studies which have suggested the need for explicit contralateral connections in the neural control of biped locomotion.

8 Acknowledgments

The author would like to thank Dr. Rolf Pfeifer and Fumiya Iida for their input on this work.

References

- [1] Bongard, J. and C. Paul Making Evolution an Offer It Can't Refuse: Morphology and the Extradimensional Bypass, in *Proc. Sixth European Conference on Artificial Life*, Prague, CZ. (2001)
- [2] Brown, T. G. On the nature of the fundamental activity of the nervous centers; together with an analysis of the conditioning of rhythmic activity in progression, and a theory of the evolution of function in the nervous system. *Journal of Physiology*, London **48**:18-46 (1914)
- [3] Dietz, V., Colombo, G. and L. Jensen. Locomotor activity in spinal man. *Lancet*, **344**:1260 (1994)
- [4] Grillner, S. Neurological Bases of Rhythmic Motor Acts in Vertebrates *Science*, **228**:143 (1985)
- [5] Kimura, H., Fukuoka Y., Konaga K., Hada Y. and K. Takase Towards 3D Adaptive Dynamic Walking of a Quadruped Robot on Irregular Terrain by Using Neural System Model in *Proc. Int. Conf. on Intelligent Robots and Systems*, Maui, USA, Oct (2001)
- [6] Matsuoka, K. Sustained oscillations generated by mutually inhibiting neurons with adaptation. *Biological Cybernetics*, **52**:367-376 (1985)
- [7] Matsuoka, K. Mechanisms of frequency and pattern control in neural rhythm generators *Biological Cybernetics*, **56**:345-353 (1987)
- [8] Ogihara, N. and Yamazaki, N. Generation of human bipedal locomotion by a bio-mimetic neuro-musculo-skeletal model *Biological Cybernetics*, **84**:1-11 (2001)
- [9] Paul, C. and J. C. Bongard The Road Less Travelled: Morphology in the Optimization of Biped Robot Locomotion, in *Proc. Int. Conf. on Intelligent Robots and Systems* Maui, Hawaii, USA, 2001
- [10] Shik, M. L., Severin, F. V. and Orlovskii G. N. Control of walking and running by means of electric stimulation of the midbrain *Biofizika*, **11**:659, 1966
- [11] Taga, G., Yamaguchi Y. and H. Shimizu. Self-organized control of bipedal locomotion by neural oscillators in unpredictable environment In *Biological Cybernetics*, 65, pages 147-159, 1991.
- [12] Thelen, E. and L. B. Smith A Dynamic Systems Approach to the Development of Cognition and Action MIT Press, 1994
- [13] Williamson, M. M. Rhythmic Robot Arm Control Using Oscillators, In *Proc. of IEEE/RSJ Int. Conf. on Intelligent Robots and Systems* Victoria, pp.77-83, (1998)